optical contact angle measurements and drop contour analysis to determine surface energy as well as interfacial and surface tension

force tensiometry, dynamic contact angle measurements, and force of adhesion evaluation

optical turbidity, stability and aging analysis of multi-phase dispersions

zeta potential measurements of fibres, powders, and plate-shaped solids

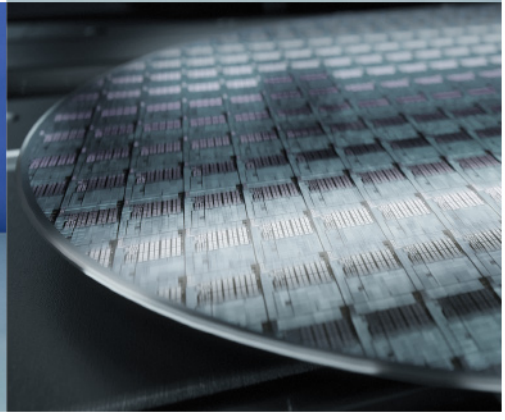

High-end, versatile laboratory measurement device portfolio for a comprehensive analysis of surfaces and interfaces

Learn more >

dataphysics
Understanding Interfaces

DataPhysics Instruments GmbH
Raiffeisenstraße 34 • 70794 Filderstadt, Germany
phone +49 (0)711 770556-0 • fax +49 (0)711 770556-99
sales@dataphysics-instruments.com
www.dataphysics-instruments.com

ADVANCED FUNCTIONAL MATERIALS
www.afm-journal.de

A Gd-Film Thermomagnetic Generator in Resonant Self-Actuation Mode

*Joel Joseph, Erika Fontana, Thibaut Devillers, Nora M. Dempsey, and Manfred Kohl**

Thermomagnetic generation is a promising technology for conversion of low-grade waste heat into electricity. Key requirements for the development of efficient thermomagnetic generators (TMGs) are tailored thermomagnetic materials as well as innovative designs enabling fast heat transfer. Recently, film-based thermomagnetic generators are developed that operate in the mode of resonant self-actuation enabling high frequency and stroke of a movable cantilever and, thus, efficient conversion of thermal energy into electrical energy. Here, the performance of a Gadolinium (Gd)-film-based TMG that is optimized for resonant self-actuation near room temperature is reported. The Gd-film TMG exhibits large oscillation frequencies up to 106 Hz and large strokes up to 2 mm corresponding to 38% of the oscillating cantilever's length. This performance occurs in a sharply bound range of ambient temperatures with an upper limit near the film's ferromagnetic to paramagnetic transition temperature T_c of 20 °C and of heat source temperatures ranging between 40 and 75 °C. The maximum power per footprint is 23.8 μWcm^{-2}, at which the Gd film undergoes a temperature change of only 0.9 °C at ≈10 °C above T_c.

1. Introduction

Thermal energy is a practically unused energy resource, even though it is abundant. A vast amount of heat rejected from energy consumption in urban and industrial sectors is lost to the environment as waste heat. Much of the unrecovered waste heat energy is in the low-temperature regime below 250 °C.[1–3] However, when temperature differences become small, conventional methods of energy generation and recovery are not possible with reasonable efficiency. The only mature technology at low temperatures is thermoelectric energy generation,[4,5] which, however, suffers from low power output, particularly at miniature scales and temperatures below 100 °C. Conversion of this low-grade thermal energy into usable energy with high efficiency is a major challenge that requires new scalable technologies.

Recently, significant progress has been made in thermomagnetic energy generation, which makes use of a temperature-dependent change of magnetic ordering due to a reversible phase transition. Promising thermomagnetic materials should exhibit a large magnetization M as well as a large change of magnetization $\Delta M/\Delta T$ within a narrow temperature window.[6] Relative efficiencies of high-performance ferromagnetic materials like Gadolinium (Gd) operating near their ferromagnetic to paramagnetic transition temperature Tc reach theoretical values up to 55% of Carnot efficiency[7] or even 73% in the case of regeneration.[8] Thermomagnetic generators (TMGs) either convert heat directly into electrical energy or indirectly via the generation of mechanical work.[9] Other concepts make use of combinations of thermomagnetic and pyroelectric effects[10] or hybrid thermomagnetic effects.[11] Macro-scale demonstrators have been presented based on ferromagnetic materials like Gd,[12–14] Heusler alloys,[15,16] and Lanthanum-Iron-Silicon (La-Fe-Si)-based alloys.[17–20] However, the efficiency of current thermomagnetic materials and conceptual devices is well below the theoretical optimum.

Film-based TMGs are designed for operation at the miniature scale,[21] which is particularly attractive for emerging applications in the field of Internet of Things (IoT) requiring self-sustaining micro sensor systems and autonomous electronic devices.[22,23] The large surface-to-volume ratio of magnetic films and supporting structures allows for efficient heat transfer. For cantilever-based devices, the concept of resonant self-actuation has been introduced giving rise to large deflections of the cantilever front and high frequencies and, thus, to large power output.[24] Recent demonstrators based on Heusler alloy films of Ni-Mn-Ga showed resonance frequencies in the order of 100 Hz and reached power densities of up to 120 mW cm^{-3}.[24,25] The typical footprint of the demonstrator devices is 10–13 mm^2, which is highly attractive for hybrid integration into microelectronic systems. However, owing to the ferromagnetic transition temperature Tc of the Ni-Mn-Ga films being ≈98 °C, the range of usable heat source temperatures was limited to 100–170 °C.[24–26] In order to apply the concept

J. Joseph, M. Kohl
Institute of Microstructure Technology
Karlsruhe Institute of Technology
Postfach 3640, D-76021 Karlsruhe, Germany
E-mail: manfred.kohl@kit.edu

E. Fontana, T. Devillers, N. M. Dempsey
Université Grenoble Alpes
CNRS
Grenoble INP
Institut Néel
Grenoble 38000, France

The ORCID identification number(s) for the author(s) of this article can be found under https://doi.org/10.1002/adfm.202301250.

DOI: 10.1002/adfm.202301250

of resonant self-actuation for recovery of low-grade thermal energy, other suitable thermomagnetic film materials need to be developed showing Tc near room temperature.[27] Promising candidates include Gd films that exhibit a Tc near room temperature, a large magnetization M under moderate magnetic field and a large temperature-dependent change of magnetization $\Delta M/\Delta T$. The possibility to easily remove them from the substrate on which they are deposited facilitates their integration into devices.[28] Environmental issues with the mining and recycling of Gd have been addressed in literature.[29,30] In the case of Gd-film TMGs, the environmental impact is considered to be rather limited due to the small amount of Gd material.

In this investigation, we develop the design and fabrication process of a miniature-scale Gd-film TMG device operating in resonant self-actuation mode and investigate its coupled physical performance properties near room temperature for decreasing heat source temperatures from 75 °C down to 35 °C. The experimental study of dynamic mechanical and electrical performance is complemented by lumped element simulations of thermal performance to elucidate the detailed processes of heat intake and heat dissipation by conduction and convection during thermo-mechanical cycling.

We demonstrate that our Gd-film TMG operates in resonant self-actuation mode down to much lower heat source temperatures of 40 °C compared to previous Ni-Mn-Ga-film TMG devices. Our device achieves a power per footprint of up to 23 μW cm^{-2}, which outperforms state-of-the-art TMGs in this temperature range. This performance is enabled by the fast heat transfer of the Gd film resulting in high frequency up to 106 Hz. The temperature change and the consumed heat of the Gd film are 0.45–1.2 °C and 0.57–0.8 Jg^{-1}, respectively, which are the lowest reported values for TMGs up to now and translate into enhanced efficiency. These results are a major milestone towards the development of TMG devices making use of low-grade waste heat near room temperature.

2. Material Properties

The active material used in the present work is a Gd film of thickness 40 μm. **Figure 1**a shows typical temperature-dependent magnetization characteristics for applied magnetic field values between 0.1 and 0.5 T. For increasing temperature, a large abrupt change of magnetization ΔM occurs within a narrow temperature window ΔT caused by a ferromagnetic to paramagnetic phase transition at the Curie temperature Tc. Due to its second order nature, the transition is hysteresis-free. An Arrott plot analysis of isothermal M(T) measurements gives a Tc value of 20 °C, in agreement with the value reported for bulk Gd.

The temperature-dependent change of magnetization $\Delta M/\Delta T$ is plotted in Figure 1b. The point of maximum $\Delta M/\Delta T$ exhibits a small field-dependent shift from 17 °C at 0.1 T to 19 °C at 0.5 T. The large change of $\Delta M/\Delta T$ of up to 2.3 Am^2 kg^{-1} K^{-1} near room temperature is the major motivation to develop a Gd film-based generator in this work. In the following, the abrupt change of magnetization will be used to generate an electrical current in a pick-up coil according to Faraday's law. Thereby, magnetic fields are typically below 0.5 T.

3. Operation Principle and Fabrication

The operation principle of the Gd-film TMG is illustrated in **Figure 2**. Major components of the TMG are a freely movable double-beam cantilever of Cu-Zn with the Gd film and a pick-up coil mounted on opposite faces of the cantilever front. A samarium cobalt (SmCo) permanent magnet is positioned above the cantilever. Owing to its double-beam design, the cantilever can be used for direct electrical connection of the pick-up coil at the cantilever front. The permanent magnet generates a magnetic field gradient force (hereafter referred to as the "magnetic attraction force") on the Gd film and, at the same time, it serves as the heat source. Therefore, in the low temperature state, the cantilever and Gd film deflect

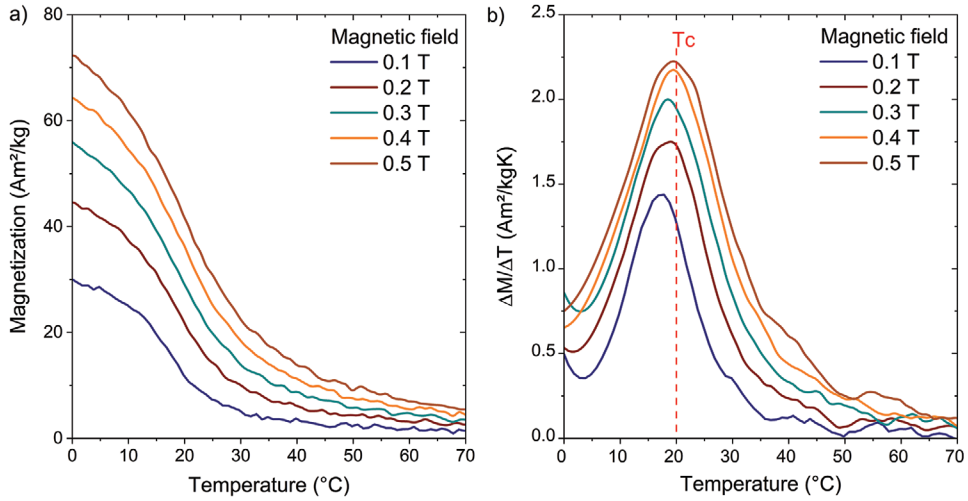

Figure 1. Thermo-magnetic properties of a Gd film of 40 μm thickness measured under various values of applied magnetic field. a) Magnetization M versus temperature T characteristics, b) temperature-dependent change of magnetization $\Delta M/\Delta T$ determined by the first derivative of the measurement data in (a).

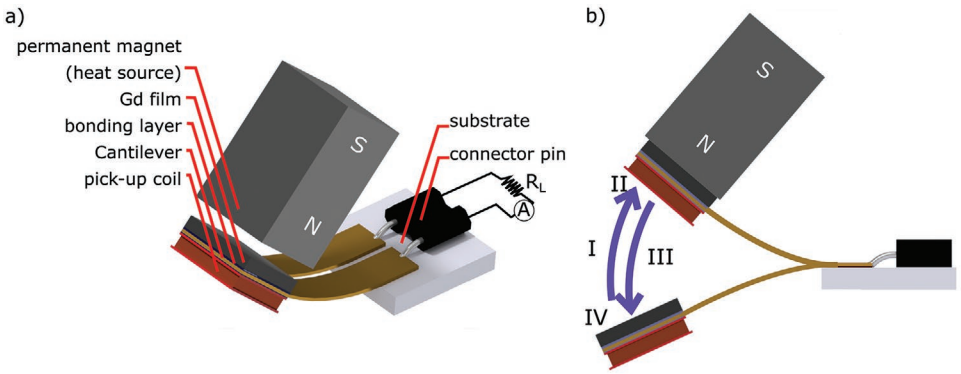

Figure 2. Schematic layout and operation principle of a Gd-film TMG. a) Layout consisting of a double-beam cantilever of Cu-Zn, bonding layer, Gd film and pick-up coil; a heatable permanent magnet is placed above the freely movable cantilever end. b) Operation principle showing four different stages of mechanical oscillation cycle: I–deflection towards the heated magnet due to magnetic attraction, II–heating due to mechanical contact to heat source, III–backward deflection due to elastic reset force of the cantilever, IV–cooling due to heat conduction and convection.

towards the magnet (I) due to magnetic attraction caused by the strong gradient of the magnetic field. Once in contact with the magnet (II), heat is transferred to the Gd film, which causes a temperature increase and a corresponding drop in magnetization. Consequently, restoring elastic and inertia forces take over to retract the cantilever from the magnet. As the cantilever moves back (III), the magnetic field and field gradient is reduced, and, at the same time, the Gd film temperature decreases due to heat conduction through the cantilever via the bonding layer of the film and forced heat convection in ambient air. At maximum deflection (IV), the restoring elastic force pulls the cantilever back again. The restoring motion is supported by the inertia and magnetic attraction force, which increases with decreasing Gd film temperature. Thus, the cantilever performs a continuous thermo-magnetic cycle (I–IV) during its oscillatory motion. Thereby, the magnetic field experienced by the Gd film ranges from a maximum of ≈0.52 T at minimum distance to the magnet (II) to a minimum of ≈0.14 T at maximum distance (IV). The actual thermo-magnetic cycle deviates from ideal conditions, as steps I and III are not adiabatic. The Gd film starts to cool as soon as it retracts from the magnet and continues to cool once the magnet attracts it again. The rapid changes of magnetization in the Gd film and of magnetic field induce a current in the pick-up coil according to Faraday's law, whereby the contribution from the film magnetization is below 5%. Under optimum conditions, the periodic deflection of the cantilever transitions to resonant self-actuation mode resulting in large oscillation stroke and high frequency as detailed in the following sections. Energy generation in the pick-up coil causes additional electromagnetic damping of the oscillatory motion, which needs to be compensated by the change of magnetic attraction force during the cycle to sustain resonant self-actuation.

Figure 3a illustrates the process sequence for fabrication of the Gd-film TMG. The starting substrate material is an alumina plate of 630 µm thickness. The double-beam cantilever is laser cut from a thin Cu-Zn foil of 30 µm thickness and attached to the substrate using a non-conductive bonding layer (I). Subsequently, a pick-up coil of 400 turns is integrated on the lower side of the cantilever front (II). The Gd film is laser cut to an area of 2×2 mm^2 and then mounted on the upper side of the cantilever front using a non-conductive bonding layer (III). Finally, the connecting link between the beams at the cantilever back is removed before a connector socket is attached to the TMG and the pins are electrically connected to the cantilever (IV). Figure 3b shows a photo of the TMG device without the magnet. The freely movable length of the cantilever is 5.3 mm, while the overall footprint is 12.6 mm^2. A SmCo magnet of $3 \times 3 \times 8$ mm^3 size with high maximum operating temperature (350 °C) is selected for device operation, which is used at the same time as a heat source. The magnetic easy axis of the magnet is aligned along its long axis.

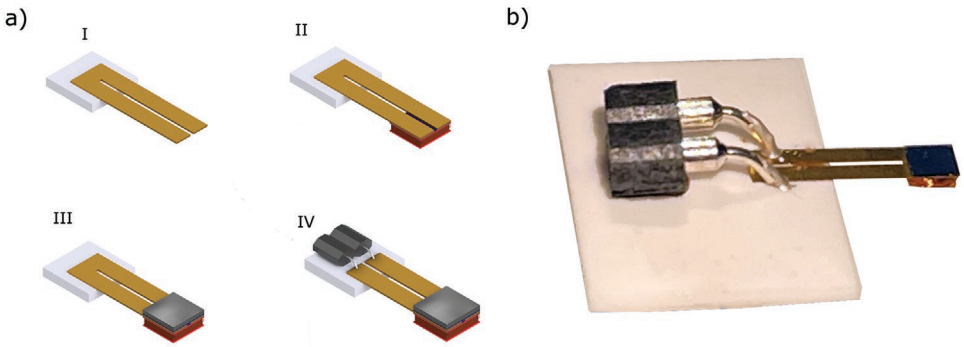

Figure 3. Schematic of fabrication process of the Gd-film TMG. a) Sequence of process steps: I–integration of cantilever on ceramic substrate, II–integration of pick-up coil, III–bonding of Gd film, IV–TMG device after electrical contacting; b) photo of final device.

Further details on fabrication and experimental procedures can be found in Section 9.

4. Performance Characteristics at Resonant Self-Actuation

Generally, self-actuation of the cantilever is governed by the interplay of magnetic attraction, elastic, inertia, and damping forces. Under non-optimized conditions, the thermal duty cycle of the film is considerably longer than the duration of the cantilever eigenoscillations. In this case, after heat intake at the heat source, the eigenoscillations decay as a function of time due to dissipation until the magnetic attraction force recovers after sufficient cooling time of the film. However, matching of the thermal duty cycle and mechanical oscillation time can be achieved if the losses in amplitude are compensated by the gain in attraction force during oscillation. Thus, resonant self-actuation occurs, if heat intake and heat dissipation are balanced and the resulting temperature change of the film ΔT causes a sufficiently large change of magnetization ΔM. Under resonant conditions, time-resolved deflections of the cantilever front with large strokes (**Figure 4**a) and high frequencies (Figure 4b) are observed. Remarkably, the range of source temperatures T_{source} at which resonant self-actuation occurs is sharply bound. For the case of 11 °C ambient temperature shown in Figure 4, resonant self-actuation sets in at ≈40 °C and, when further increasing the source temperature, it stops abruptly at ≈71 °C. Within this temperature range, the stroke stays above 1.5 mm and exhibits a maximum of 2 mm at 60 °C. The frequency, on the other hand, starts at rather low values of 65 Hz, gradually increases up to 106 Hz at 65 °C, and then abruptly declines at the critical maximum source temperature. This performance of stroke and frequency correlates with the power output shown in Figure 4c. At the lower limit of heat source temperature of 40 °C, the power is already 1.3 µW corresponding to a power per footprint of 10.3 µW cm^{-2} (8.1 mW cm^{-3} power per Gd volume), which is about the highest value observed for Gd-based TMGs at low-temperature difference between heat source and ambient (T_{source}–T_{amb}) of only 29 °C. For increasing source temperature, the power first increases gradually and then strongly until the maximum power of 3 µW occurs at 65 °C corresponding to a power per footprint of 23.8 µW cm^{-2} (18.8 mW cm^{-3}). In these measurements, the load resistance of the electrical circuit has been set to its optimal value of ≈500 Ω. This value is higher than the internal resistance of the pick-up coil of ≈220 Ω. As detailed in (Figure S1, Supporting Information), the power further increases when increasing the load resistance beyond 220 Ω, as the reduction in electromagnetic damping results in a further increase of stroke and frequency.

5. Temperature Range of Resonant Self-Actuation

For most applications, operation near room temperature is desirable. Therefore, it is essential to investigate the range of ambient temperatures T_{amb}, at which resonant self-actuation occurs for the given Gd film. **Figure 5** gives an overview on actuation strokes, oscillation frequencies, and electrical power output in the range of ambient temperatures T_{amb} between 9 and 19 °C. Thereby, the source temperature T_{source} has been varied between 35 and 75 °C. The following observations can be made:

– The range of ambient temperatures T_{amb}, at which resonant self-actuation occurs, is sharply bound in all cases. The TMG is capable of sustaining resonant self-actuation for increasing

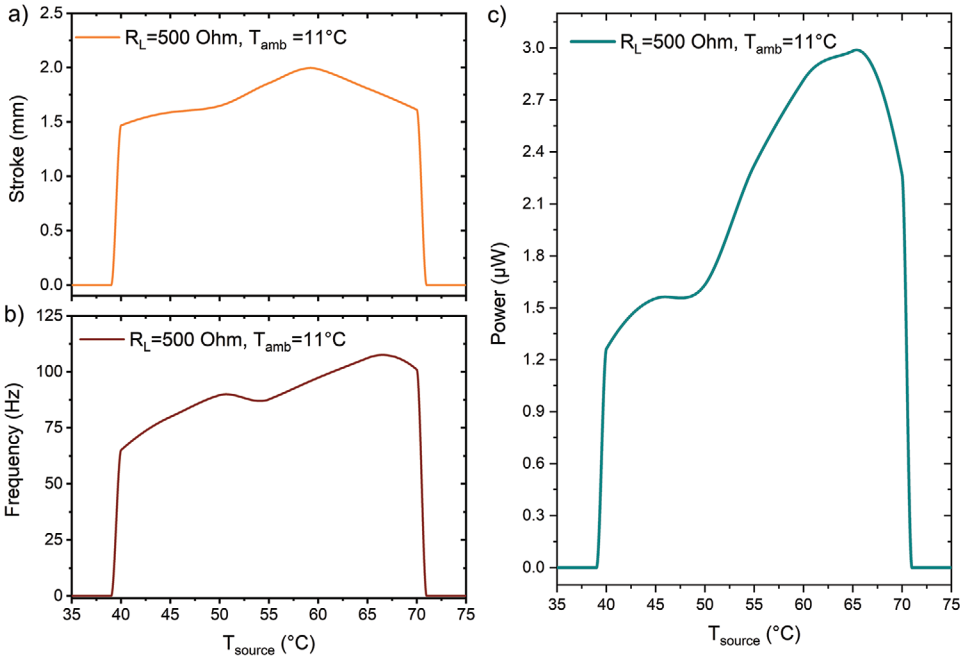

Figure 4. Mechanical and electrical performance of the Gd-film TMG as a function of heat source temperature (T_{source}) at an ambient temperature (T_{amb}) of 11 °C: a) Stroke of the cantilever front during resonant self-actuation, b) oscillation frequency of cantilever front, c) electrical power output measured from the induced current of the pick-up coil at a load resistance of 500 Ω.

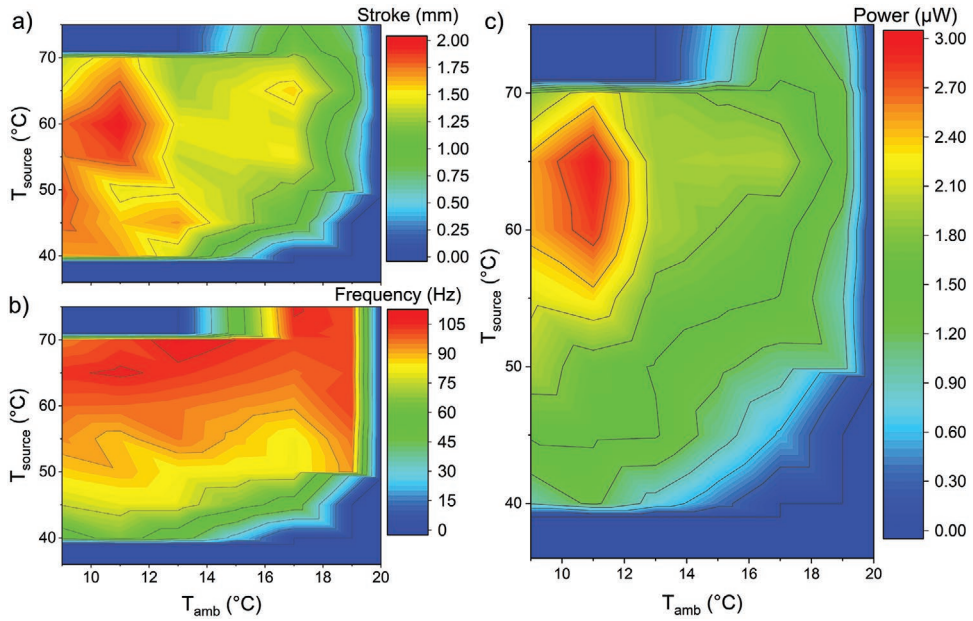

Figure 5. Experimental results on the mechanical and electrical performance of the TMG device as a function of ambient temperature (T_{amb}) and heat source temperature (T_{source}). Numerical values can be inferred from the given color code. A summary of numerical values is also provided in Table S1 (Supporting Information). a) Stroke of the cantilever front during resonant self-actuation, b) oscillation frequency of cantilever front, c) electrical power output measured from the induced current of the pick-up coil at a load resistance of 500 Ω.

T_{amb} up to 19 °C, while at 20 °C and above resonant self-actuation is no longer possible. At 19 °C, the TMG device still generates ≈1 μW at T_{source} of 50 °C and 1.4 μW at T_{source} of 65 °C.

- At lower ambient temperatures T_{amb} < 19 °C, the lower and upper limits of allowable source temperatures are shifting towards higher values roughly as T_{amb} is increasing, i.e., from 40 °C < T_{source} < 70 °C at T_{amb} of 9 to 50 °C < T_{source} < 75 °C for increasing T_{amb} by 10 °C.
- The maximal stroke of ≈2 mm occurs at T_{amb} of 11 °C. For increasing T_{amb}, the stroke drops continuously reaching a minimum value of 800 μm at 19 °C.
- The frequency is almost unaffected by the change of T_{amb} within the resonance region. However, at low source temperature T_{source}, frequencies are low (see Section 4) and tend to further decrease for increasing T_{amb} until resonant self-actuation stops.
- A pronounced maximum power point occurs at T_{amb} of 11 °C, which coincides with the maximum stroke and frequency at source temperature T_{source} between 55 and 70 °C.

Further overview plots on the mechanical and electrical performance of the TMG device are summarized as a function of load resistance and heat source temperature at different ambient temperatures in Figures S1–S6 (Supporting Information). In addition, a summary of numerical values is provided in Table S1 (Supporting Information).

6. Analysis of Thermal Performance

The large power output observed during resonant self-actuation is enabled by efficient conversion of thermal energy via magneto-mechanical energy into electrical energy. Therefore, at first, a detailed understanding of the heat transfer dynamics is required to identify key thermal design parameters and to optimize their effect on the conversion of thermal energy. In the following, a validated lumped element model (LEM, SIMSCAPE R-2021b, 2021, MATLAB) is introduced to analyze the thermal performance of the TMG. The LEM and simulation procedure has been adapted from previous work for the actual double-beam cantilever design and material parameters of the Gd film.[27] The LEM model has been validated by comparing experimental performance data on time-dependent actuation stroke, frequency, induced electrical current, and corresponding power output. The dynamics of heat intake during mechanical contact between the Gd film and the heat source, and of subsequent heat dissipation through heat conduction and convection are simulated. Thereby, the heat transfer coefficient κ at contact is used as an adjustment parameter. The resulting temperature change of the Gd film is then used to calculate the change of magnetic attraction force and the resulting mechanical performance. The modeling parameters are summarized in Table S2 (Supporting Information). Figure S8 (Supporting Information) shows, for instance, experimental and simulated time-resolved characteristics of cantilever deflection and induced electrical current. Within the experimental error estimated to be below 5%, the simulated time-resolved characteristics describe well the experimental results.

Figure 6 gives an overview on simulated heat intake, heat dissipation due to conduction and convection as well as corresponding temperature changes in the Gd film in the investigated range of ambient temperatures T_{amb} and source temperatures T_{source}. The heat intake shown in Figure 6a correlates with the heat source temperature T_{source}. At low ambient temperatures, the largest heat intake occurs ranging from 70 mW

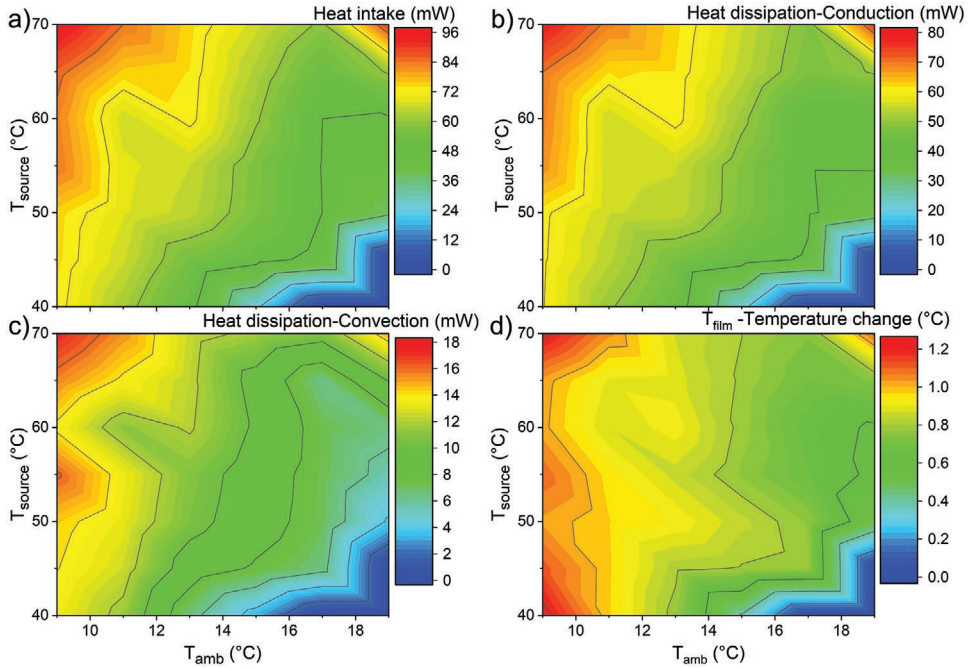

Figure 6. Simulation results on the thermal performance of the TMG device as a function of ambient temperature (T_{amb}) and heat source temperature (T_{source}). Numerical values can be inferred from the given color code. A summary of numerical values is also provided in Table S1 (Supporting Information). a) Heat intake during mechanical contact between the Gd film and the heat source, b) heat dissipation due to heat conduction from the Gd film via a non-conductive bonding layer to the cantilever, c) heat dissipation due to heat convection from the Gd film to the ambient air, d) resulting average temperature change of the Gd film T_{film}.

at T_{source} of 40 °C to 97 mW at T_{source} of 70 °C. For increasing ambient temperature, the heat intake decreases. Thus, minimum values of ≈40 mW are found at the ambient temperature of 19 °C. The key parameter governing heat intake is the heat transfer coefficient κ at contact between the Gd film and the heat source. LEM simulations reveal that κ should be as large as possible. At least, a minimal heat transfer coefficient is required, above which stable resonant oscillation occurs characterized by large stroke and frequency.[31] In the present case, the required minimal heat transfer coefficient κ is determined to be ≈4000 $Wm^{-2}K^{-1}$ by matching the measured electrical and mechanical performance of the TMG with the LEM simulations, which is in line with our previous simulations[31] and literature data.[32]

The simulated heat dissipation from the Gd film by heat conduction to the cantilever via the bonding layer (Figure 6b) shows the same dependencies on T_{amb} and T_{source} as the heat intake. In particular, the largest heat dissipation by heat conduction occurs at low ambient temperatures, ranging from 60 mW at T_{source} of 40 °C to 79 mW at T_{source} of 70 °C. Comparing these numbers with the heat intake, the heat conduction accounts for the largest fraction of heat dissipation. Thus, the cantilever acts as the major heat sink. The heat dissipation from the Gd film by heat convection to the ambient air correlates with the stroke and frequency of oscillation and, hence, dependencies on T_{amb} and T_{source} differ from the heat intake to some extent (Figure 6c). Nevertheless, the heat dissipation by conduction and convection is matching the simulated heat intake indicating overall consistency of the results. The key parameter governing conductive heat dissipation is the thermal resistance R_b of the bonding layer between the Gd film and the cantilever.[31] This value requires adjustment during the design of the TMG device to match heat intake during contact with the heat source for optimal heat transfer.

Owing to the rather large oscillation frequency and corresponding short heat transfer times, the resulting temperature changes shown in Figure 6d are rather small varying between 1.2 °C at low ambient temperatures T_{amb} of 9 °C and ≈0.45 °C at T_{amb} of 19 °C. This result is remarkable, as only a fraction of a degree in temperature change ΔT appears to be sufficient to enable stable operation under resonant self-actuation conditions.

As the cantilever acts as the major heat sink, the cantilever temperature T_{cant} is another important thermal parameter. **Figure 7**a shows the simulated cantilever temperature T_{cant} in the investigated range of ambient and source temperatures. The value of T_{cant} increases for increasing ambient temperature T_{amb} and source temperatures T_{source}. Minimal values of T_{cant} are ≈25 °C, while maximum values reach 34 °C. The increase in T_{cant} causes a reduction in heat dissipation of the Gd film, which consequently limits the heat intake as well. Therefore, the increase in T_{cant} for increasing ambient temperature T_{amb} correlates with the reduction in heat dissipation and in heat intake shown in Figure 6.

At the optimum power point (T_{amb} = 11 °C, T_{source} = 65 °C), the cantilever temperature T_{cant} is determined to be 28.4 °C. In this case, the film temperature T_{film} varies in time between ≈28.5 and 29.4 °C (ΔT = 0.9 °C) as shown in Figure 7b. The corresponding time-resolved heat intake (Figure 7c) occurs in short pulses within ≈0.5 ms with each pulse corresponding to

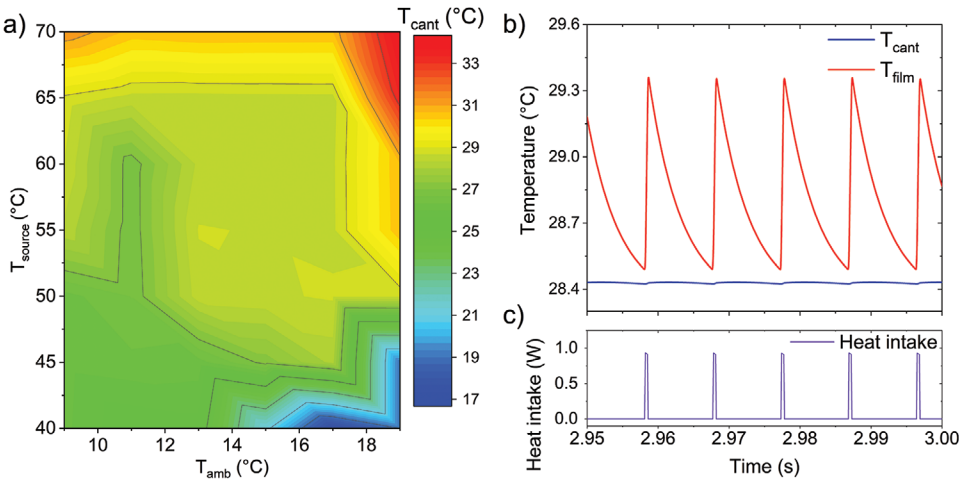

Figure 7. a) Simulation results on the average cantilever temperature T_{cant} in the investigated range of ambient temperature (T_{amb}) and heat source temperature (T_{source}), b) time-dependent change of temperature of the Gd film (T_{film}) and of the corresponding cantilever temperature T_{cant}, at the optimum power point (T_{amb} = 11 °C and T_{source} = 65 °C), c) corresponding time-dependent change of heat intake of the Gd film at contact with the heated magnet.

the time of contact between the Gd film and the heated magnet. Subsequent cooling occurs within ≈9 ms. This performance may be compared with the lower limit of operation at ambient temperature T_{amb} of 19 °C and source temperature T_{source} of 50 °C. In this case, the cantilever temperature T_{cant} is almost the same (28.6 °C), but the film temperature T_{film} only varies by 0.45 °C. Our results indicate that this value of ΔT is a lower limit for resonant self-actuation. In this case, the corresponding change of magnetization ΔM drops below a critical limit, below which the magnetic attraction force can no longer compensate for damping losses.

7. Discussion

Film-based TMGs can operate in the mode of resonant self-actuation enabling high frequency and stroke and, thus, efficient conversion of thermal into electrical energy. However, the range of usable heat source temperatures is higher than the ferromagnetic to paramagnetic transition temperature Tc of the used thermomagnetic material, e.g., 100–170 °C for a Ni-Mn-Ga film with Tc of ≈98 °C at 0.5 T.[26] Therefore, suitable thermomagnetic films need to be developed and implemented having a critical temperature Tc near room temperature. Promising material candidates include Gd which has a Tc of 20 °C. Here, we investigate the coupled thermo-magneto-mechanical performance of a Gd-film TMG near room temperature for decreasing heat source temperatures from 75 °C down to 35 °C to assess its potential for recovery of low-grade waste heat.

For the TMG design, we use a validated LEM simulation model as described in detail by Joseph et al.[27] It involves an adjustment of the resonance frequency by the cantilever dimensions, the optimization of heat intake by the dimensions of contact area between film and heated magnet, the matching of heat dissipation via the bonding layer between film and substrate as well as matching of load resistance. The LEM is used to investigate the conditions for resonant self-actuation as well as to identify the optimal performance parameters for maximum power and efficiency during resonant self-actuation at maximum possible ambient temperature.

Film-based TMG devices show self-adapting performance, i.e., the frequency and amplitude of resonant self-actuation vary as a function of the ambient and heat source temperatures and, thus, the devices can operate in resonant self-actuation mode at different levels of heat transfer.[24,25] However, our investigation of a Gd-film TMG reveals a sharply bound range of ambient and source temperatures required for resonant self-actuation. The upper limit of ambient temperature T_{amb} coincides with the temperature at which $\Delta M/\Delta T$ is maximum (19 °C at 0.5 T), while at 20 °C and beyond resonant self-actuation is no longer possible independent of heat source temperature T_{source}. At the limit of T_{amb} = 19 °C, TMG devices are still capable to generate ≈1 µW at the minimum and maximal heat source temperatures of 50 and 75 °C, respectively. At lower ambient temperature T_{amb} of 11 °C, for instance, resonant self-actuation abruptly sets in already at 40 °C, whereby a power output of 1.3 µW is obtained. The corresponding relative power per footprint of 10.3 µW cm^{-2} (8.1 mW cm^{-3} power per Gd volume) is about the highest value observed for Gd-based TMGs at low-temperature difference between heat source and ambient of only 29 °C. When further increasing T_{source}, resonant self-actuation stops abruptly beyond ≈71 °C. At T_{source} of 40 °C, the efficiency given by the ratio of electrical output power and intake of thermal power is ≈0.0021%. The corresponding relative efficiency given by the ratio of absolute and Carnot efficiency is estimated to be 0.045% assuming that the cantilever temperature is the heat sink temperature as it accounts for ≈80% of heat dissipation. The corresponding Gd film material's efficiency is determined to be 0.02%. It is given by the ratio of output magnetic energy and thermal input energy, whereby the output magnetic energy is determined from the thermomagnetic cycle of the Gd film shown in Figure S9 (Supporting Information). The concept of resonant self-actuation does not rely on using the full temperature range of the magnetic transition for energy conversion, but on a minimum possible temperature change of the film

ΔT_{film} to achieve the maximum electrical power output instead of optimal efficiency. The efficiency is lower compared to TEG devices at similar ΔT. Furthermore, operation conditions are highly dynamic and far from stationary conditions. In this case, an appropriate performance metric is the ratio of electrical power output and intake of thermal power.

The Gd-film TMG is optimized for operation at maximum possible ambient temperature and exhibits a pronounced maximum power point at an ambient temperature T_{amb} of 11 °C, which coincides with the maximum stroke and frequency at the heat source temperatures between 55 and 70 °C. The maximum power is ≈3 µW corresponding to a power per footprint of 23.8 µW cm^{-2} (18.8 mW cm^{-3}). Our thermal analysis indicates that the Gd film temperature varies in this case by 0.9 °C at ≈10 °C above the film's ferromagnetic transition temperature Tc. At this temperature, the temperature-dependent change of film magnetization $\Delta M/\Delta T$ under 0.5 T is 1.4 Am^2 kg^{-1} K^{-1} and, thus, the corresponding change of magnetization ΔM is determined to be ≈1.3 Am^2 kg^{-1}. While optimal heat transfer dynamics are important to sustain resonant self-actuation, the ambient and source temperatures causing maximum heat transfer do not coincide with the corresponding temperatures causing maximum power output. This can be explained by the complex dependency of power not only on the heat transfer dynamics but also on the mechanical and electrical performances. Thus, optimizing power does not require the largest heat intake or temperature change within the material, but rather optimal heat intake and temperature change enabling highest frequency and stroke.

We can identify three limiting cases for operation of the Gd-film TMG defining its sharply bound operation range: 1) an upper limit of ambient temperature T_{amb}^{max} of 19 °C for all heat source temperatures T_{source}, 2) a lower limit of source temperature T_{source}^{min} between 40 and 50 °C, and 3) an upper limit of source temperature T_{source}^{max} between 70 and 75 °C, whereby specific values of T_{source}^{min} and T_{source}^{min} depend on ambient temperature T_{amb}. The lower limit of ambient temperature is not investigated here, as the focus is on the potential of waste heat recovery near room temperature.

Case 1): At maximum ambient temperature T_{amb}^{max} of 19 °C, the temperature change ΔT of the Gd film during a mechanical oscillation cycle reaches a minimal value, below which the change of magnetization ΔM (Figure 1b) and corresponding change in magnetic attraction force become too low to compensate for losses during oscillation. For instance, at the source temperature, T_{source} of 50 °C, ΔT is only 0.45 °C (28.7 °C < T_{film} < 29.15 °C) causing a low magnetization change ΔM below 0.6 Am^2 kg^{-1}. At the source temperature T_{source} of 70 °C, T_{film} varies by ≈1.1 °C (34.2 °C < T_{film} < 35.3 °C). However, at these elevated film temperatures, the temperature-dependent change of magnetization $\Delta M/\Delta T$ is reduced by more than a factor of 2 (Figure 1b), and, therefore, the lower limit of ΔT is already reached at a correspondingly higher value. Below these limits of ΔT, resonant self-actuation is no longer possible.

Case 2): At the lower limit of source temperature T_{source}^{min} the oscillation frequency reaches a lower limit, below which the mechanical and thermal duty cycles get out of balance. This performance results from too low heat intake due to the low-temperature difference between source and film temperature. For instance, the frequency reaches its lowest value of 52 Hz at T_{source}^{min} of 40 °C. In this case, the heat intake is only 51 mW. Consequently, resonant self-actuation becomes unstable despite the relatively large change of magnetization ΔM under 0.5 T of ≈1.5 Am^2 kg^{-1}.

Case 3): At the upper limit of source temperature T_{source}^{max}, the cantilever temperature T_{cant} reaches an upper limit, above which the mechanical and thermal duty cycle gets out of balance. As discussed in Section 6, the cantilever acts as the major heat sink. Therefore, the increase of T_{cant} leads to overheating due to limited heat dissipation. For instance, at T_{source} of 70 °C, the cantilever temperature reaches 31 °C at T_{amb} of 9 °C and even 34 °C at T_{amb} of 19 °C.

Figure 8 gives an overview of operation frequency, temperature change ΔT, and power per footprint for selected TMG devices having different sizes and operating at different heat source temperatures. Only TMG devices are considered for comparison, for which an electrical power output and the dimensions have been reported. Film-based TMGs rely on mechanical contact between film and heat source for heat intake and on heat dissipation via the oscillating cantilever. In this case, the large surface-to-volume ratio of the film allows for a large frequency of operation being typically in the range of 50 to 200 Hz.[24,25] Therefore, film-based TMGs exhibit much higher frequencies compared to devices using bulk TMG materials operating at a few Hz only. Comparing the temperature change ΔT of the used thermomagnetic materials (Figure 8b), ΔT values of the Gd-film TMGs of 0.45–1.2 °C are the lowest reported for TMGs up to now. Low values of ΔT are desirable as a low amount of thermal energy is sufficient for power generation. For film-based TMGs operating in resonant self-actuation mode, minimum ΔT values depend on the temperature-dependent change of magnetization $\Delta M/\Delta T$ of the used material. Recent work on TMGs based on Heusler alloy Ni-Mn-Ga films revealed typical values between 3 and 10 °C.[25] Other TMGs using bulk thermomagnetic materials are operated at even higher ΔT values, typically between 30[17] and 80 °C.[33] In particular, bulk Gd and La-Fe-Co-Si materials have been investigated in macro-scale TMG devices with an optimized magnetic circuit to directly convert the change of magnetization into electrical current using a heat transfer fluid for heat exchange between thermo-magnetic material and heat source/sink.[20] In this case, TMGs using Gd showed a lower power output compared to La-Fe-Co-Si, which has been ascribed to losses due to magnetic stray fields originating from its unsymmetrical magnetization versus temperature characteristics. However, such conditions do not apply to Gd-film TMGs that operate at lowest ΔT values under dynamic, resonant self-actuation conditions to achieve optimal power output. In Figure 8c, we compare the power per footprint of the TMGs taking the size dependence of power output into account. The power per footprint of the Gd-film TMG of 23.8 µW cm^{-2} is among the largest values reported for TMGs operating below 100 °C. Even at 40 °C, the Gd-film TMG achieves a power per footprint of 10.3 µW cm^{-2}. Larger values up to 50 µW cm^{-2} have been achieved for TMGs based on Heusler alloy Ni-Mn-Ga films operating between 130 and 170 °C.[25] A maximum power per footprint of 3.1 µW cm^{-2} has been reported for a TMG based on Gd bulk material[20] and 31.7 µW cm^{-2} for a TMG based on La-Fe-Co-Si.[17] However, in these cases, the

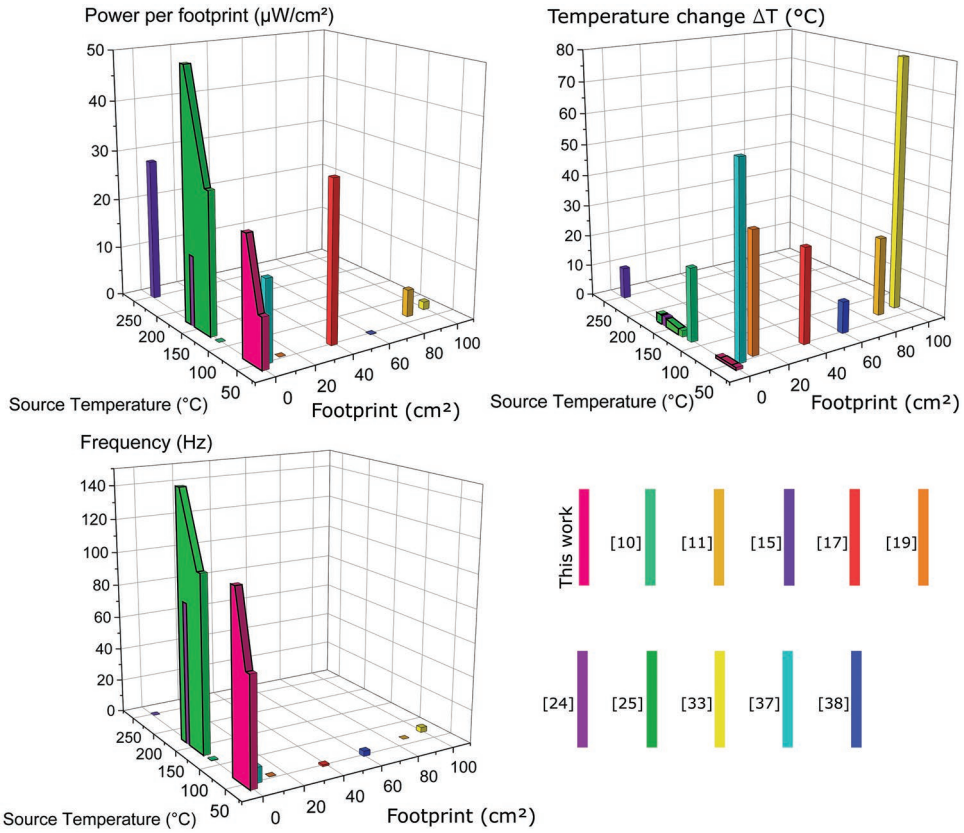

Figure 8. Benchmarking against other thermomagnetic energy harvesters for low-grade harvesting with electrical outputs. References: Lallart et. al.[10] Rodrigues et. al.[11] Srivastava et.al.[15] Waske et. al.[17] Ahmim et. al.[19] Gueltig et. al.[24] Joseph et. al.[25] Chun et. al.[33] Chun et. al.[37] Carlioz et.al.[38]

power consumption and size of the pumping system used for heat transfer have not been taken into account. Therefore, the power per footprint of our device outperforms state-of-the-art TMGs in the temperature range near room temperature. The high performance of the Gd-film TMGs is enabled by the concept of resonant self-actuation allowing for very low device footprint of 12.6 mm^2, operation at high frequency, and lowest temperature change of the thermomagnetic material down to 0.45 K.

When comparing the power densities with TEG devices, the temperature difference and length scale should be taken into account, as it defines the applicability and competitiveness.[24] The power output of the Gd-film TMG compares well with state-of-the-art TEG devices at the mm-length scale, if the size of the heat sink is taken into account. For comparison, see, e.g.,[34,35] This is due to limitations in microfabrication of the μ-TEGs, which strongly limits ΔT requiring large heat sinks that exceed the size of the TEG module by far (see, e.g.,[36]).

A detailed account of economic properties of TM materials is given in ref. [6]. For a Gd material cost of 20 € kg^{-1}, the cost index of the Gd film has been estimated to be 8 € W^{-1}. This estimate does not include the costs of processing and shaping, as these costs depend on the scale of production. As pointed out in ref. [6], while material cost will hinder bulk application, this is not the case with microsystem applications. In this case, processing costs will be the dominant factor, which strongly depends on chip size and footprint.

8. Conclusions

We present a Gd-film-based TMG that has been developed and optimized for resonant self-actuation near room temperature. The 40 μm thick Gd film is fabricated by triode sputtering and shows a large magnetization M exceeding 70 $Am^2\ kg^{-1}$ at 0.5 T and a corresponding maximum temperature-dependent change of magnetization $\Delta M/\Delta T$ of 2.3 $Am^2kg^{-1}K^{-1}$ at 19 °C. A detailed experimental and LEM simulation study is presented to assess the coupled thermo-magneto-mechanical performance of the Gd-film TMG near room temperature. When operating in resonant self-actuation mode, the TMGs exhibit high operation frequencies up to 105 Hz due to the large surface-to-volume ratio of the Gd film. Thereby, the Gd film undergoes a very low-temperature change ΔT of 0.4–1.2 K. The large oscillation stroke and frequency result in high power per footprint up to 23.8 μW cm^{-2}. In this case, the Gd film temperature varies by 0.9 °C at ≈10 °C above T_c. The device performance strongly depends on the balance of heat intake and heat dissipation, which are determined by the heat transfer coefficient at contact between the Gd film and the heat source and by the thermal resistance of the bonding layer between the Gd film

and the cantilever, respectively, acting as the major heat sink. Resonant self-actuation of the Gd-film TMG occurs in a sharply bound temperature range, which is determined by three limiting cases. 1) The upper limit of ambient temperature occurs near the film's ferromagnetic to paramagnetic transition temperature T_c of 20 °C, above which the temperature change ΔT of the Gd film and, thus, the corresponding change in magnetic attraction force becomes too low to compensate for losses during oscillation. 2) The lower limit of source temperature is reached at ≈30 K above ambient temperature, below which heat intake becomes too low and, thus, mechanical and thermal duty cycles get out of balance. 3) The upper limit of source temperature is caused by overheating when heat intake can no longer be balanced by heat dissipation.

The TMG devices are well suited for powering microelectronic devices due to their ability to actively generate air circulation to cool themselves in a confined space without the need for any heat sink to maintain the temperature gradient. The fabrication process of the Gd-film TMG outlined in the Experimental Section is compatible with MEMS technology including sputtering of the TM film and hybrid integration of the TM film and pick-up coil by transfer bonding, which can be easily combined with microelectronic fabrication technology. The power output in the μW range will be sufficient to render sensors, watches, and IoT devices independent of batteries. Depending on the target application, power levels can be adapted by arranging the TMG devices in an array for operation in parallel. As the Gd film is exposed to low strain at the cantilever, long life is expected. This has been confirmed by running the TMG device at ≈100 Hz for 3 d without any degradation corresponding to more than 25 million cycles.

In this work, the investigated Gd-film TMG serves as a demonstrator system to investigate TMG performance in resonant self-actuation mode at heat source temperatures near room temperature. Specific applications will require further efforts in materials development and engineering. So far, the upper limit of ambient temperature of 19 °C limits the application range. Performance improvements are expected in particular by tailoring the thermomagnetic film materials with respect to slightly higher values of T_c and larger temperature-dependent changes of magnetization $\Delta M/\Delta T$. Our results indicate that increasing the ferromagnetic transition T_c by ≈2 °C will enable resonant self-actuation at room temperature, which could be achieved, e.g., by developing Boron-doped Gd films.[39] Enhancing $\Delta M/\Delta T$ will enable further reduction of the lower limit of source temperature to enable recovery of low-grade thermal energy below 40 °C at room temperature. This will open the door for novel self-powered medical devices using the temperature difference between body and room temperature.

9. Experimental Section

The Gd film was fabricated by triode sputtering of a Gd target of 3N purity onto a rotating Si substrate of diameter 100 mm, heated at 400 °C.[40] The Gd layer was protected by Ta buffer and capping layers of thickness 100 nm, also deposited at 400 °C. Thanks to the elevated temperature of deposition, the Ta/Gd/Ta trilayer could be easily peeled from the Si substrate.[28,40] X-ray diffraction (XRD) confirmed the hcp crystallographic structure of the Gd layer (data not shown). Magnetic characterization of the Gd film was performed using an extraction magnetometer.

A pulsed laser was used to structure the alumina substrate having a thickness of 630 μm. The cantilever design consists of two parallel beams, whereby the beams at the cantilever back were connected by a link for parallel beam alignment. The lateral dimensions were designed to be 0.9 × 5.3 mm^2. Fabrication was performed by laser precision cutting of a Cu-Zn foil of 30 μm thickness. The micromachined cantilevers were then attached to a ceramic substrate using a non-conductive bonding layer. The pick-up coil consists of a polymethylmethacrylate (PMMA) core with dimensions of 1 × 1 × 0.25 mm^3 and outer end caps made of a 50 μm thick Kapton foil with lateral dimensions of 2 × 2 mm^2. They consist of 400 turns of an enamel-coated copper wire of 15 μm diameter fabricated using an in-house built semi-automatic coil winder. The two ends of the copper wire were bonded to the two cantilever tips using an electrically conductive bonding layer. The pick-up coil was bonded to the front end of the cantilever using a non-conductive bonding layer by sandwiching the electrical contact of the pick-up coil between the pick-up coil and the cantilever. The Gd film was laser cut to an area of 2 × 2 mm^2 and then mounted on the upper side of the cantilever front using a non-conductive epoxy bonding layer. A bonding layer thickness of 18 μm was used, which corresponds to a thermal resistance of 20 K W^{-1}. Finally, the connecting link between the beams at the cantilever back was removed before a connector socket was attached to the TMG and the pins were electrically connected to the cantilever. A permanent magnet of SmCo of 3 × 3 × 8 mm^3 size was mounted above the cantilever using a custom-made holder. Beforehand, the magnet surface was polished to a mirror finish using sandpaper to optimize heat transfer at contact between the Gd film and the magnet. A resistive heater was integrated in the holder to adjust the temperature of the magnet. Temperature control was realized using an RTD sensor (PT 100) attached near the tip of the magnet. The dissipated power of the heat source has been matched to the mass of the magnet. The RTD sensor was connected to a temperature sensor module USB-TEMP from MCC and InstaCal software was used to process the temperature data. The ambient temperature was maintained by cooling down the entire laboratory room to maintain the large thermal heat sink and was monitored using two thermocouples, one close to the setup and one further away to make sure that the temperature was similar throughout the experiment.

The measurement setup consisted of precision stages that allow for aligning the TMG device with respect to the magnet to maximize thermal contact during operation. A laser triangulation sensor from Panasonic (Panasonic HL-G103SJ) was used for deflection measurements. The sensor was used in Analog mode by connecting it to a USB 6211 A/D card from National Instruments. Since the cantilever was bending upwards, it undergoes a 2D motion, which causes an error of ≈5% between measured and actual stroke. A load resistor was connected to the TMG to measure the electrical output of the device. The electrical current through the load resistor was determined using a current pre-amplifier from Stanford Research Systems (Model SR570) connected in series. A sensitivity of 100 μA V^{-1} was chosen, which allows for a resolution of 60 pA under a low noise setting. The output of the current pre-amplifier was also connected to an USB 6211 A/D card and a PC. Data recording and initial data processing was performed by using LabVIEW, which involves the calculation of instantaneous power from the measured current. A python script was used to analyze the data to calculate average power by integrating instantaneous power for the entire time and dividing it by the duration of data acquisition. The stroke was calculated by doing a peak-to-peak analysis of deflection measurement data and averaging over the entire measurement. FFT analysis was used to determine the operation frequency from time-resolved deflection measurements. Power, stroke, and frequency were calculated for 10 measurements taken consecutively and then the mean values were calculated to obtain the average values of power, stroke and frequency at each measurement point.

Supporting Information

Supporting Information is available from the Wiley Online Library or from the author.

Acknowledgements

This work was funded by the German Science Foundation (DFG) through the "Thervest II" project (KO2953/6-3) and the French National Research Agency through the "HiPerTher-Mag" project (ANR-18-CE05-0019). This work was partly carried out with the support of the Karlsruhe Nano Micro Facility (KNMFi, www.knmf.kit.edu).

Open access funding enabled and organized by Projekt DEAL.

Conflict of Interest

The authors declare no conflict of interest.

Data Availability Statement

The data that support the findings of this study are available from the corresponding author upon reasonable request.

Keywords

energy harvesting, gadolinium films, magnetic materials, thermomagnetic energy generation, waste heat recovery

Received: February 3, 2023
Published online:

[1] R. A. Kishore, S. Priya, *Renewable Sustainable Energy Rev.* **2018**, *81*, 33.
[2] A. N. Bucsek, W. Nunn, B. Jalan, R. D. James, *Annu. Rev. Mater. Res.* **2020**, *50*, 283.
[3] A. Kitanovski, *Adv. Energy Mater.* **2020**, *10*, 1903741.
[4] J. L. Bierschenk, in *Energy Harvesting Technologies*, (Eds: S. Priya, D. J. Inman), Springer US, Boston, MA **2009**.
[5] G. Min, in *Energy Harvesting for Autonomous Systems*, (Eds: S. P. Beeby, N. White), Artech House, Norwood, Mass **2010**.
[6] D. Dzekan, A. Waske, K. Nielsch, S. Fähler, *APL Mater.* **2021**, *9*, 011105.
[7] L. Brillouin, H. P. Iskenderian, *Thermomagnetic Generator. Electronic Communications* **1948**, *25*, 300.
[8] L. D. Kirol, J. I. Mills, *J. Appl. Phys.* **1984**, *56*, 824.
[9] R. A. Kishore, S. Priya, *Materials* **2018**, *11*, 1433.
[10] M. Lallart, L. Yan, H. Miki, G. Sebald, G. Diguet, M. Ohtsuka, M. Kohl, *Appl. Energy* **2021**, *288*, 116617.
[11] C. Rodrigues, A. Pires, I. Gonçalves, D. Silva, J. Oliveira, A. Pereira, J. Ventura, *Adv. Funct. Mater.* **2022**, *32*, 2110288.
[12] M. Ujihara, G. P. Carman, D. G. Lee, *Appl. Phys. Lett.* **2007**, *91*, 093508.
[13] K. P. Wetzlar, S. M. Keller, M. R. Phillips, G. P. Carman, *J. Appl. Phys.* **2016**, *120*, 244101.
[14] R. A. Kishore, D. Singh, R. Sriramdas, A. J. Garcia, M. Sanghadasa, S. Priya, *J. Appl. Phys.* **2020**, *127*, 044501.
[15] V. Srivastava, Y. Song, K. Bhatti, R. D. James, *Adv. Energy Mater.* **2011**, *1*, 97.
[16] A. Post, C. Knight, E. Kisi, *J. Appl. Phys.* **2013**, *114*, 033915.
[17] A. Waske, D. Dzekan, K. Sellschopp, D. Berger, A. Stork, K. Nielsch, S. Fähler, *Nat. Energy* **2019**, *4*, 68.
[18] S. Ahmim, M. Almanza, A. Pasko, F. Mazaleyrat, M. LoBue, *The European Physical Journal Applied Physics* **2019**, *85*, 10902.
[19] S. Ahmim, M. Almanza, V. Loyau, F. Mazaleyrat, A. Pasko, F. Parrain, M. LoBue, *J. Magn. Magn. Mater.* **2021**, *540*, 168428.
[20] D. Dzekan, A. Diestel, D. Berger, K. Nielsch, S. Fähler, *Sci. Technol. Adv. Mater.* **2021**, *22*, 643.
[21] M. Gueltig, H. Ossmer, M. Ohtsuka, H. Miki, K. Tsuchiya, T. Takagi, M. Kohl, *Adv. Energy Mater.* **2014**, *4*, 1400751.
[22] J. W. Matiko, N. J. Grabham, S. P. Beeby, M. J. Tudor, *Meas. Sci. Technol.* **2014**, *25*, 012002.
[23] R. Vullers, R. Schaijk, H. Visser, J. Penders, C. Hoof, *IEEE Solid-State Circuits Magazine* **2010**, *2*, 29.
[24] M. Gueltig, F. Wendler, H. Ossmer, M. Ohtsuka, H. Miki, T. Takagi, M. Kohl, *Adv. Energy Mater.* **2017**, *7*, 1601879.
[25] J. Joseph, M. Ohtsuka, H. Miki, M. Kohl, *Joule* **2020**, *4*, 2718.
[26] M. Kohl, M. Gueltig, F. Wendler, *Shape Memory and Superelasticity* **2018**, *4*, 242.
[27] J. Joseph, M. Ohtsuka, H. Miki, M. Kohl, *Materials* **2021**, *14*, 1234.
[28] D. Nguyen Ba, Y. Zheng, L. Becerra, M. Marangolo, M. Almanza, M. LoBue, *Phys. Rev. Appl.* **2021**, *15*, 064045.
[29] T. Dutta, K. H. Kim, M. Uchimiya, E. E. Kwon, B. H. Jeon, A. Deep, S. T. Yun, *Environ. Res.* **2016**, *150*, 182.
[30] K. Binnemans, P. T. Jones, B. Blanpain, T. van Gerven, Y. Yang, A. Walton, M. Buchert, *J. Clean Prod.* **2013**, *51*, 1.
[31] J. Joseph, M. Ohtsuka, H. Miki, M. Kohl, *iScience* **2022**, *25*, 104569.
[32] R. Karwa, *Heat and Mass Transfer*, 2nd ed., Springer Nature, Singapore **2017**.
[33] J. Chun, H.-C. Song, M.-G. Kang, H. B. Kang, R. A. Kishore, S. Priya, *Sci. Rep.* **2017**, *7*, 41383.
[34] W. Wang, V. Cionca, N. Wang, M. Hayes, B. O'Flynn, C O'Mathuna, *Int. J. Distrib. Sens. Netw.* **2013**, *9*, 232438.
[35] M. Strasser, R. Aigner, C. Lauterbach, T. F. Sturm, M. Franosch, G. K. M. Wachutka, *Sens Actuators A Phys* **2004**, *114*, 362.
[36] K. B. Joshi, S. Priya, *Smart Mater. Struct.* **2013**, *22*, 055005.
[37] J. Chun, R. A. Kishore, P. Kumar, M.-G. Kang, H. B. Kang, M. Sanghadasa, S. Priya, *ACS Appl. Mater. Interfaces* **2018**, *10*, 10796.
[38] L. Carlioz, J. Delamare, S. Basrour, *TRANSDUCERS 2009 –2009 International Solid-State Sensors, Actuators and Microsystems Conference*, IEEE, Piscataway, NJ **2009**.
[39] W. Dunhui, H. Songling, H. Zhida, S. Zhenghua, W. Yi, D. Youwei, *Solid State Commun.* **2004**, *131*, 97.
[40] E. Fontana, Universitê Grenoble Alpes, **2022**.